

Oxygen and aluminum diffusion in α -Al₂O₃: How much do we really understand?

A.H. Heuer*

Department of Materials Science and Engineering, Case Western Reserve University, Cleveland, OH 44106, USA

Available online 1 February 2008

Abstract

The major diffusion processes in α -Al₂O₃ have been reviewed, including oxygen and aluminum lattice diffusion, D_{oxy} and D_{Al} , respectively; oxygen grain boundary diffusion, $D_{\text{b-oxy}}$; and pipe diffusion, D_{p} . Their relevance to creep of Al₂O₃ and oxidation of Al₂O₃ scale-forming alloys is briefly considered.

It is concluded that the answer to the question included in the title is “not a great deal”. Eight major questions and issues have been identified that would constitute fitting subjects for future research:

- (i) What is the nature of the “buffering” that appears to control D_{oxy} ?
- (ii) What process(es) are occurring during annealing that eliminate non-Fickian behavior when measuring D_{oxy} ?
- (iii) How should the magnitude of the measured activation energies for D_{oxy} be interpreted?
- (iv) Have all the defect types involved in oxygen diffusion been identified?
- (v) Does oxygen diffusion occur by an interstitialcy mechanism?
- (vi) What is the order of magnitude of $D_{\text{Al}}/D_{\text{oxy}}$?
- (vii) What is the order of magnitude of $D_{\text{b-Al}}/D_{\text{b-oxy}}$?
- (viii) It appears that the activation energy for $D_{\text{b-oxy}}$ is greater than that for D_{oxy} . How should this be understood?

© 2008 Published by Elsevier Ltd.

Keywords: B. Defects; B. Grain Boundaries; C. Diffusion; D. Al₂O₃

1. Introduction

Self-diffusion of oxygen and aluminum in Al₂O₃ has been of scientific and technological interest for nearly half a century. Alumina in both single crystal and polycrystalline form is arguably *the* most important structural ceramic, and knowledge of lattice, grain boundary, and pipe diffusion is crucial for understanding a host of important high temperature processes: plastic deformation of single crystals, diffusional creep and sintering of polycrystals, oxidation of Al₂O₃-scale forming alloys, etc. (Al₂O₃ scales provide the very best oxidation resistance for structural alloys in oxidizing environments.) Furthermore, Al₂O₃ is often considered a model material for many oxide ceramics and other refractory non-metallic substances, and the

database of its properties, fabrication, and areas of application is probably unequaled among modern ceramics.

This writer had earlier pointed out¹ the difficulty of understanding the activation energy for oxygen lattice diffusion in Al₂O₃ in the context of traditional point defect chemistry considerations (“Oxygen diffusion in corundum (α -Al₂O₃): a conundrum”, *Philos. Mag. Lett.* **79** p. 629 (1999)). In this paper, a tribute to Sir Richard Brook on the occasion of his 70th birthday, this issue is revisited. Some considerations of pipe diffusion and grain boundary diffusion are also included, as well as some brief comments on the applicability of these data to diffusional creep of alumina and oxidation of Al₂O₃-scale forming alloys. Attention is restricted to the stable corundum polymorph, α -Al₂O₃, with space group $R\bar{3}c$.

In addition to the conundrum regarding the activation energy for lattice diffusion¹ (the values deduced for the migration energy, about 5 eV, are very much larger than the calculated migration energies, which are of the order of 1.5–2.0 eV^{2,3}); it

* Tel.: +1 216 368 3868; fax: +1 216 368 8932.
E-mail address: heuer@case.edu.

is concluded that there are major difficulties in understanding: (i) the processes that occur during annealing of single crystal specimens prior to diffusion experiments that eliminate non-Fickian behavior; (ii) whether the lattice diffusivities of oxygen and aluminum are similar or not; (iii) the magnitude of the pre-exponential and activation energy for oxygen grain boundary diffusion in alumina polycrystals; and (iv) the defects and defect equilibria controlling oxygen diffusion in this scientifically interesting and technologically important material. It turns out that we do not understand a great deal about diffusion in $\alpha\text{-Al}_2\text{O}_3$!

2. Oxygen diffusion

2.1. Lattice diffusion

Oxygen self-diffusion in Al_2O_3 single crystals and polycrystals was first measured in 1960 using gaseous exchange of ^{18}O -enriched oxygen by Oishi and Kingery,⁴ who annealed Verneuil-grown single crystal spheres, crushed Verneuil rods, and crushed polycrystals which had been sintered at 1900°C . Some of the latter were made into spherical particles by dropping through a three-phase carbon arc. After the ^{18}O diffusion anneal, the amount of ^{18}O exchange was determined from mass spectrometric measurement of gas samples taken intermittently during the exchange, or by reducing the exchanged oxide to CO by heating with graphite to 1700°C , catalytically converting the CO to CO_2 , and determining the $^{48}\text{CO}_2/^{44}\text{CO}_2$ ratio. Although significant variability was observed, the authors thought they had observed “intrinsic” diffusion at elevated temperatures ($>1650^\circ\text{C}$) and an “extrinsic” regime at lower temperature. The parameters, D_0 and Q , of the Arrhenius equation describing this data are included in Table 1 and plotted in the standard format in Fig. 1. Enhanced diffusion was observed for the polycrystalline specimens, as is also shown in Fig. 1.

Oishi et al.^{5,6} extended these measurements using the oxide reduction/mass spectroscopy technique to crushed particles of a high purity CVD-grown single crystal, to Verneuil-grown 3.2 mm sapphire rod cut into $200\ \mu\text{m}$ thick discs and buff polished with $1\ \mu\text{m}$ diamond paste,⁵ to similar discs prepared from high purity CVD grown material,⁵ and to $800\ \mu\text{m}$ thick discs prepared from 3.2 or 4.0 mm Verneuil-grown sapphire rods that had been chemically polished or Ar-ion-milled.⁶ These data were interpreted as suggesting that the “extrinsic” region shown in Fig. 1 was due to dislocation-enhanced oxygen diffusion, the defects arising from the crushing operation, and by inference, that the chemically polished or Ar-ion-milled data were the most reliable. The diffusion activation energies were in tolerable agreement with the “intrinsic” values of Oishi and Kingery (see Table 1 and Fig. 1).

Oxygen diffusion in undoped sapphire has since been studied by several groups in the USA, France, and Japan using either SIMS (Secondary Ion Mass Spectroscopy)^{7–11} or NRA (Nuclear Reaction Analysis) involving the $^{18}\text{O}(\text{p},\alpha)^{15}\text{N}$ reaction^{8,12} to determine ^{18}O depth profiles following high temperature

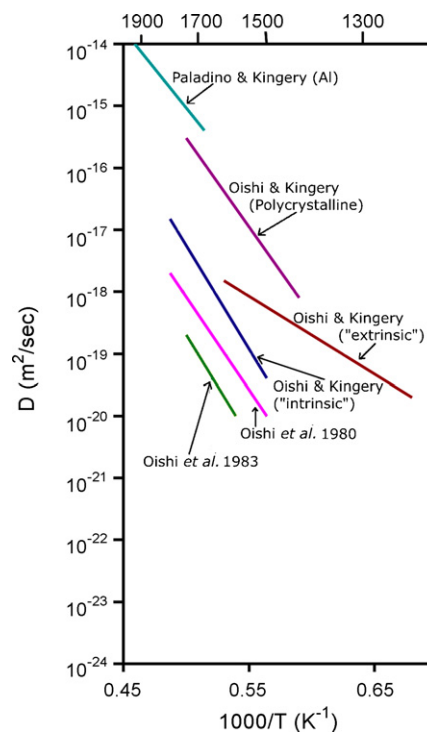


Fig. 1. Early data on lattice oxygen and aluminum diffusion in $\alpha\text{-Al}_2\text{O}_3$ by Oishi and Kingery,⁴ Paladino and Kingery,⁵⁵ and Oishi et al.,^{5,6} and on oxygen diffusion in Al_2O_3 polycrystals.⁴ The temperature scale at the top of this and subsequent figures is in $^\circ\text{C}$.

exchange with ^{18}O -enriched oxygen. Lastly, Lagerlöf et al.¹³ inferred oxygen self-diffusion coefficients from measurements of the shrinkage of small prismatic dislocation loops in sapphire crystals that had previously been deformed at 1400°C . (The diffusion coefficient of the slower (rate-controlling) specie, oxygen or aluminum, was actually determined, and it was assumed that $D_{\text{Oxy}} < D_{\text{Al}}$ under all conditions.)

These measurements on nominally undoped sapphire are included in Table 1 and shown in Fig. 2, along with the 1983 data of Oishi et al.⁶ In spite of the considerable experimental difficulties involved in determining D_{Oxy} in single crystal Al_2O_3 , due to the very low absolute magnitudes of the oxygen diffusivities, the several different techniques and diverse origins of the single crystals used by Japanese, French, and American investigators, the fact that SIMS and NRA determination of the ^{18}O profiles, and hence of D_{Oxy} , of the same crystals could disagree by a factor of 2^{12} , and most importantly, the expectation that uncontrolled impurities, especially aliovalent dopants, would significantly affect diffusion kinetics,^{1,13} there is reasonably good agreement of the data (generally within ~ 1 order of magnitude). The most recent Japanese studies by Nakagawa, Ikuhara and co-workers^{10,11} involved high purity Czochralski and high purity Verneuil crystals. ICP-AES analysis of the Czochralski crystal revealed 2.8 ppmw Ti, with Ca, Mg, Na, K, Fe, Ba, Zr, Mo, W, Mn, and Cd being present in amounts below the detection limits, whereas a total of 30 ppm cation and 16 ppm anion impurities were present in the Verneuil crystal. The new Japanese data are in very good agreement with

Table 1

Arrhenius parameters, D_0 and Q , for diffusive processes in α -Al₂O₃ ($D = D_0 \exp(-Q/RT)$)

Oxygen Lattice Diffusion (undoped), D_{oxy}	D_0 (m ² /s)	Q (kJ/mol)
Oishi and Kingery (“intrinsic”)	3.0×10^{-1}	641
Oishi and Kingery (polycrystalline)	6×10^{-2}	548
Oishi and Kingery (“extrinsic”)	6.3×10^{-12}	239
Oishi, Ando, and Kubota, 1980	7.4×10^{-4}	573
Oishi, Ando, Suga, and Kingery, 1983	5.0×10^{-3}	628
Reed and Wuensch	9.3×10^2	795
Reddy and Cooper	3.2×10^{-1}	653
Cawley, Halloran and Cooper	1.5×10^{-2}	601
Prot and Monty	2.6×10^{-3}	603
Lagerlöf, Mitchell and Heuer	6.8×10^{-4}	588
Nakagawa, Nakamura, Sakaguchi, Shibata, Lagerlöf, Yamamoto, Haneda, and Ikuhara	8.0×10^{-6}	532
Nakagawa, Sakaguchi, Shibata, Matsunaga, Mizoguchi, Yamamoto, Haneda, and Ikuhara	4.6×10^{-4}	567
Oxygen Lattice Diffusion (doped), D_{oxy}	D_0 (m ² /s)	Q (kJ/mol)
Reddy and Cooper (Ti-doped)	2.0×10^{-3}	536
Reddy and Cooper (Mg-doped)	3.5×10^{-1}	655
Reddy thesis (Mg-doped from Al ₂ O ₃ polycrystals)	2.5	625
Lagerlöf, Mitchell and Heuer (Ti-doped)	2.6×10^{-2}	674
Lagerlöf, Mitchell and Heuer (Mg-doped)	4.7×10^{-3}	559
Haneda and Monty (Ti-doped)	1.6×10^{-2}	635
Haneda and Monty (Mg-doped)	2.0×10^6	844
Aluminum Lattice Diffusion, D_{Al}	D_0 (m ² /s)	Q (kJ/mol)
Paladino and Kingery	3.6×10^{-4}	482
LeGall, Lesage, and Bernardini	5.0×10^4	281
Oxygen Grain Boundary Diffusion, $D_{\text{b-oxy}}\delta$	D_0 (m ³ /s)	Q (kJ/mol)
Reddy thesis (undoped)	5.5×10^1	825
Prot, LeGall, and Lesage (undoped)	1.2×10^2	884
Prot, LeGall, and Lesage (Y-doped)	1.2×10^{-3}	780
Messaoudi, Huntz, and Lesage	2.1×10^1	391
Clemens, Bongartz, Quadackers, Nickel, Holzbrecher, and Becker	3.5×10^2	310
Nakagawa, Sakaguchi, Shibata, Matsunaga, Mizoguchi, Yamamoto, Haneda, and Ikuhara (undoped bicrystal)	8.4×10^{-6}	627
Nakagawa, Sakaguchi, Shibata, Matsunaga, Mizoguchi, Yamamoto, Haneda, and Ikuhara (Y-doped bicrystal)	6.5×10^{-4}	729
Pipe Diffusion, D_{p}	D_0 (m ² /s)	Q (kJ/mol)
Tang, Lagerlöf, and Heuer (undoped)	8.7×10^{-3}	439
Nakagawa, Nakamura, Sakaguchi, Shibata, Lagerlöf, Yamamoto, Haneda, and Ikuhara (undoped)	4.6×10^{-2}	464
Creep, D_{creep}	D_0 (m ² /s)	Q (kJ/mol)
Cannon, Rhodes, and Heuer	4.8×10^{-1}	444
Yoshida, Ikuhara, and Sakuma (undoped) stress exponent $n = 2$	^a	410
Yoshida, Ikuhara, and Sakuma (Y-doped) $n = 2$	^a	830
Cho, Wang, Chan, Rickman, and Harmer (undoped) $n = 2$	^a	483
Cho, Wang, Chan, Rickman, and Harmer (Y-doped) $n = 2$	^a	685

^a The D_0 parameters could not be determined from Eq. (1).

the two most recent^{9,13} prior studies. (These new data were acquired in the course of pipe diffusion and grain boundary diffusion studies, which are reviewed below.) As noted earlier,¹³ the point defect population controlling D_{oxy} appears to be strongly “buffered.”

Reed and Wuensch⁷ used a diffusion couple involving a film of Al₂¹⁸O₃ deposited on Al₂O₃ single crystals to determine D_{oxy} , rather than gaseous exchange with ¹⁸O enriched oxygen, and also performed the diffusion anneal in vacuum ($<1.3 \times 10^{-3}$ Pa) rather than in air or oxygen; their pre-exponential is very large (and probably unphysical), and their

activation energy is about 20% higher than that found by the other investigators (Table 1). Cawley et al.⁸ showed that diffusion anneals at low $p\text{O}_2$ (10^{-10} Pa) did not affect D_{oxy} , and Reddy and Cooper¹² showed that the differences observed between their data and the Reed/Wuensch data, essentially the $\sim 10\times$ lower D_{oxy} , could not be attributed to the different techniques (SIMS vs. NRA) used to determine ¹⁸O concentration profiles, or the different crystals used by the two groups. Reddy and Cooper’s suggestion that problems in temperature measurement might be the cause of the discrepancies between their data and the Reed/Wuensch data deserves serious consideration.

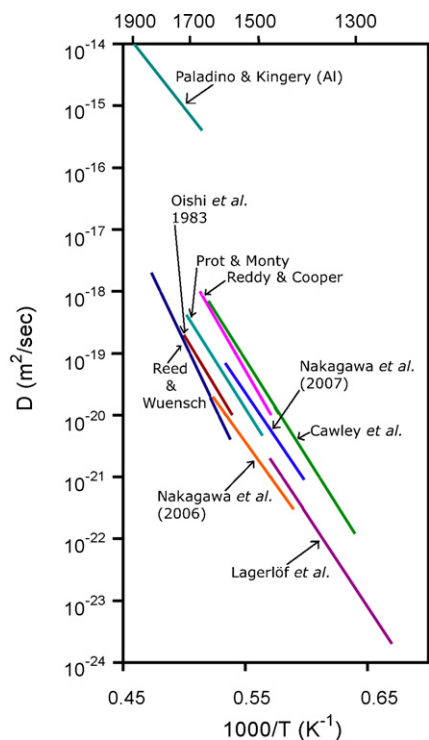


Fig. 2. SIMS,^{7–11} NRA,^{8,12} and dislocation loop shrinkage¹³ data on lattice oxygen diffusion in α -Al₂O₃.

Buffering is also an issue in the studies of crystals intentionally doped with Mg and Ti.^a Mg-doping increases D_{oxy} ^{b13,16} and Ti-doping decreases D_{oxy} ,^{12,13} although the magnitude of the increase or decrease was not consistent among the several investigations (Table 1 and Fig. 3). Doping has only modest effect on the activation energy for oxygen diffusion, and the magnitude of the changes are also relatively modest—the largest effects on D_{oxy} were reported in the loop shrinkage work,¹³ where a decrease in D_{oxy} of ~ 50 in a 600 ppm Ti-doped crystal and an increase in D_{oxy} of ~ 100 in a 250 ppm Mg-doped crystal was found. This is clearly a further result of the “buffering” just alluded to—classical point defect concepts would suggest^{1,13} that doping with these aliovalent solutes would change the concentration of the defects mediating oxygen diffusion (conventionally considered to be oxygen vacancies or oxygen interstitials), and hence the diffusivity, by many orders of magnitude, rather than by factors of 50 or 100. The question of whether oxygen diffusion occurs via a vacancy-

^a Although crystals doped with Y₂O₃ have been studied, they will not be discussed in detail, as Y apparently segregates to the surface of growing crystals during solidification¹⁴ and such crystals do not have Y contents that are as high as the concentrations of unintentional impurities introduced during crystal growth.¹⁵ Oxygen grain boundary diffusion in Y₂O₃-doped alumina polycrystals is discussed in Section 2.3.

^b Reddy and Cooper¹² did not find an effect of Mg doping on D_{oxy} , a possible result of Mg evaporation during ¹⁸O exchange.¹⁷ The Haneda and Monty¹⁶ Mg-doped data are not considered reliable because of the very large pre-exponential and activation energy; however, their Ti-doped data are in good agreement with the Reddy/Cooper Ti-doped data. Fig. 3 also contains Reddy’s data¹⁷ on oxygen lattice diffusion obtained from studies of MgO-doped polycrystalline alumina, which will be discussed further below.

type or interstitial-type mechanism is discussed in Section 2.2.

Further consideration of the problem of interpreting the lattice diffusion activation energies by Harding et al.¹⁸ did not resolve the conundrum but added a further problem, that of understanding grain boundary diffusion in Al₂O₃ polycrystals, an issue which is discussed further below.

This section is concluded by discussing a very novel theory recently offered by Doremus^{19,20} to explain diffusion in Al₂O₃ and oxidation of Al-containing alloys. Doremus accepted the aluminum self-diffusion data of Le Gall et al.²¹ (data which are problematic—see below) that self-diffusion coefficients of oxygen and aluminum in Al₂O₃ are of similar magnitude, and proposed that “bulk diffusion of oxygen (and aluminum) takes place by jumps of AlO molecules from one AlO vacancy to another.” As applied to oxidation of Al-containing alloys, the theory has been severely criticized by Pint and Deacon,²² criticism that Doremus did not accept.²³ While there are issues of physical plausibility with Doremus’ theory, he can nevertheless be lauded for attempting some new thinking on this topic.

Doremus’ novel approach was apparently motivated by the widely accepted idea that oxidation of silicon is controlled by molecular diffusion of water (in moist ambients) and O₂ molecules (in dry ambients) through the adherent SiO₂ scale.^{24,25} However, the amorphous SiO₂ scale formed during oxidation of Si is quite open (the density, ρ , is ~ 2250 kg/m³), whereas α -Al₂O₃ itself is dense and close-packed (ρ is

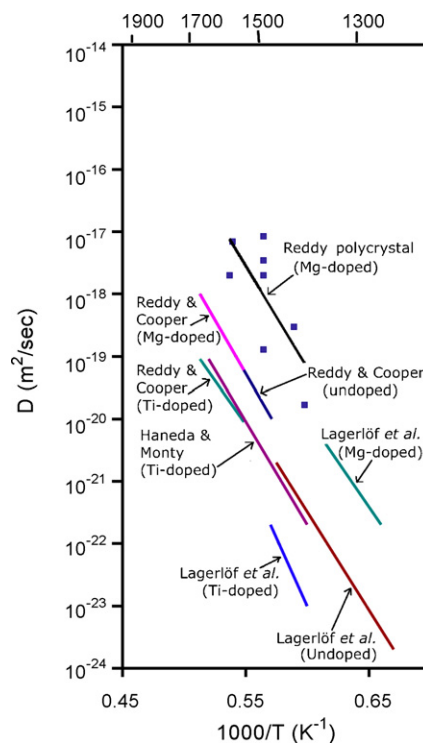


Fig. 3. Lattice oxygen diffusion data on Mg- and Ti-doped single crystal Al₂O₃,^{12,13} and Mg-doped polycrystalline¹⁷ Al₂O₃. (The Mg-doped and undoped Arrhenius curves for Reddy and Cooper’s single crystal data¹² overlap.) As Reddy’s data¹⁷ on D_{oxy} derived from Mg-doped polycrystals have not been previously published (other than in his thesis), both the data and the best fit Arrhenius plot are included.

3986 kg/m³). Thus, diffusion of AlO molecules in Al₂O₃ on steric grounds alone should be difficult.

In addition, there are at least three aspects of Doremus' proposal that are unconvincing:

- (i) that D_{Al} is of the same order of magnitude as D_{oxy} (see Section 3);
- (ii) that AlO is a viable vapor species above Al₂O₃ at elevated temperatures; and
- (iii) that neutral $(V_{Al} V_O)^x$ point defect complexes (Kröger–Vink notation) are available in high concentrations.

Lou et al.²⁶ had earlier provided an extensive review of the various vapor species above Al₂O₃ at elevated temperatures and concluded that AlO is never present in appreciable amounts as a vapor specie. Furthermore, the total pressures above alumina at the temperatures of interest (say 900–1200 °C for oxidation experiments and 1400–1800 °C for diffusion experiments) are very low.

As far as is known, neutral divacancies such as $(V_{Al} V_O)^x$ have not been considered in the several theoretical studies dealing with point defects in Al₂O₃, in large part because of the dominant ionic character of Al₂O₃. The charged divacancy $(V_{Al}''' V_O^{••})'$ had been specifically considered in the “conundrum” paper but rejected as playing any role in diffusion phenomena; this obtained because theoretical calculations²⁷ suggested that its fractional abundance would be $\sim 10^{-14}$, and thus too low to be of any importance. (Chien and Heuer²⁸ have suggested that the corresponding charged divacancy $(V_{Zr}''' V_O^{••})''$ in Y₂O₃-doped ZrO₂ controls high temperature diffusion-controlled processes in that material, for which $D_{oxy} \gg D_{Zr}$ because of the large concentration, 5–10%, of oxygen vacancies. Incidentally, the D_o and Q parameters determined by the dislocation loop shrinkage technique in Y₂O₃-doped ZrO₂ are in very good agreement with these parameters determined by SIMS experiments using ⁹⁶Zr.²⁹)

2.2. Non-Fickian behavior

This section is concerned with the effect of annealing on D_{oxy} and the related matter of the effect of damage introduced during specimen preparation and its effect on D_{oxy} . These issues, while considered in many of the previously cited papers, remain troublesome.

Oishi and Kingery,⁴ late in their experimental program, discovered that a good deal of the variability ($\pm 100\%$) in D_{oxy} they encountered could be attributed to effects of prior heat treatment, although this effect was not apparent for diffusion temperatures above 1650 °C. Oishi et al.⁵ suggested that short circuit diffusion via dislocation networks or subgrain boundaries could enhance D_{oxy} (by as much as a factor of 10), and that this effect could be eliminated by prior annealing.

Reed and Wuensch⁷ annealed their crystals for 4 h at 1650 °C before the diffusion experiments to attempt to remove damage arising from mechanical polishing. A specimen which had

not been preannealed showed a flat near-surface region in the ¹⁸O penetration profile, ~ 100 nm thick, which was attributed to enhanced diffusion arising from polishing damage. (Prior and subsequent publications^{30–35} have shown that the damaged layer arising from mechanical polishing with fine, 1 or 2 μ m, diamond abrasives is restricted to a layer ≤ 1 μ m in thickness.) Unfortunately, there have been no systematic and comprehensive TEM studies of the type pioneered by Hockey³⁰ that have characterized the damage introduced by mechanical polishing with fine diamond abrasives, and the removal of this damage by annealing; such studies would be a welcome addition to the literature.

Reddy and Cooper,¹² and Cawley et al.¹⁴ annealed their samples prior to exchange for times and temperatures comparable to those employed for the actual exchange, even when cleaved specimens were used,¹² while Prot and Monty⁹ annealed their samples at the exchange temperature for 12 h. In the most recent Nakagawa/Ikuhara SIMS studies,^{10,11} samples were annealed either at 1400 °C¹¹ or 1500 °C¹⁰ for 3 h in air prior to the diffusion anneals. Further, in all the tracer studies cited, the diffusion depths ($\sim (D_{oxy}t)^{1/2}$, where t is time) were in the range 0.1–0.6 μ m, i.e. within the zone that had been damaged by mechanical polishing. ($(D_{oxy}t)^{1/2}$ values in the study¹³ involving dislocation loop shrinkage are much smaller, but polishing damage was not an issue in that study; it was assumed that in the ion-thinned TEM foils being studied, if a dislocation loop emitted a vacancy or absorbed an interstitial during loop shrinkage, point defect equilibrium near the loop was readily reestablished in times short with respect to the duration of the diffusion anneal.

Non-Fickian behavior indicating or showing a “tail” in the ¹⁸O penetration profile was observed in the NRA study of Reddy and Cooper¹² (Fig. 4) using Verneuil, Czochralski, and Schmidt–Viechnicki crystals, and the SIMS studies of Prot and Monty,⁹ who used Verneuil crystals. (Fig. 4 was actually obtained from the Schmidt–Viechnicki crystals showing the lowest grown-in dislocation density, $\sim 10^7$ m⁻².) Reddy and Cooper reported that: (i) all unannealed samples show such non-Fickian behavior; (ii) that the tails could be reduced in magnitude by annealing but that annealing times greater than the exchange times were needed to completely eliminate such tails; (iii) that the tails could not be reintroduced by annealing in vacuum; and (iv) that the nature of the tails did not depend on the initial dislocation density of their samples, which varied from 10^7 m⁻² to 10^9 m⁻². They further pointed out that pipe diffusion alone could not account for these tails; as already noted, the magnitude of the tails did not depend on dislocation density, and unreasonably large dislocation pipes would be required to account for the deep ¹⁸O penetration.

Prot and Monty⁹ (and Le Gall et al.¹⁵) adopted a very different view. They assumed that the tails in the ¹⁸O penetration profiles in undoped (and “Y₂O₃-doped”) Verneuil crystals were due to enhanced diffusion along subboundaries (a factor of about 10^5 higher diffusivity compared to bulk diffusion), and showed one TEM image of a subboundary containing seven dislocations spaced about 300 nm apart. (This is apparently the same image published earlier by Le Gall et al.²¹ in their study of Al diffusion. For completeness, it is noted that this group¹⁵ in the study of a “Y₂O₃-doped” crystal showed a TEM image of a different sub-

boundary.) Prot and Monty reported that the activation energies, Q , for boundary diffusion was nearly 40% higher than that for bulk diffusion. Unfortunately, these investigators did not study whether more extended preannealing could eliminate the tails.

The higher activation energy reported by Prot and Monty⁹ may suggest that short circuit diffusion in Al_2O_3 does not follow the rule of thumb observed in metals, i.e. that such diffusion always display lower activation energies than those that obtain for lattice diffusion. However, as pointed out by Harding et al.,¹⁸ the pre-exponential factor, D_0 , they reported for oxygen subboundary diffusion in undoped Al_2O_3 , $3.1 \times 10^{10} \text{ m}^2/\text{s}$, is unreasonably large and cannot be reconciled with any conceivable diffusion mechanism.

Great credence is given here to Reddy and Cooper's¹² observations that the non-Fickian behavior was not sensitive to the grown-in dislocation densities in their crystals, even in crystals with densities as low as 10^7 m^{-2} , and was present in cleaved crystals which do not suffer from surface damage during specimen preparation. It is thus concluded that the "tails" observed by Prot and Monty,⁹ and Le Gall et al.¹⁵ cannot have been due to enhanced subboundary diffusion and the Arrhenius parameters they reported have not been included in Table 1. The tails must have another origin; what could this be?

One possibility is that following crystal growth, cooling to room temperature, and reheating to the temperature of the diffusion anneal, the crystals do not have the equilibrium concentration of the point defects involved in oxygen transport. The annealing effect shown in Fig. 4, and the tails in the SIMS data referred to already,^{9,15} would thus be a manifestation of the

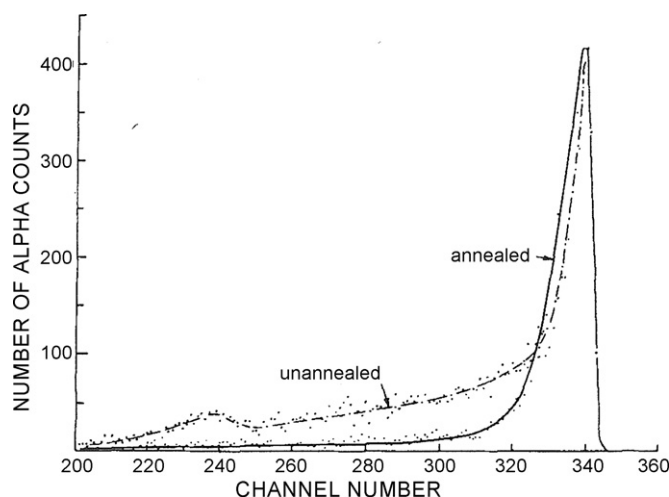


Fig. 4. "Single spectrum" NRA data showing the effect of annealing on "tails" in the ^{18}O penetration profile.¹² In these NRA experiments, monoenergetic protons (800 keV in this instance) undergo the $^{18}\text{O}(p, \alpha)^{15}\text{N}$ reaction in solids containing ^{18}O . As the protons traverse the solid, they lose energy as do the back-scattered alpha particles. Knowing the rate at which protons and alpha particles lose energy in Al_2O_3 , it is straightforward to associate each channel in the alpha particle detector to a depth beneath the surface where the exoergic (p, α) reaction occurred. The resonance in the $^{18}\text{O}(p, \alpha)^{15}\text{N}$ reaction occurs, for example, at 629 keV (channel 239); the alpha particles corresponding to this energy originated at a depth $\sim 2 \mu\text{m}$ below the surface. The alpha particle spectra are then fit to the appropriate solution to the diffusion equation. The "unannealed" spectrum cannot be fit to a "Fickian" solution to the ^{18}O penetration profile and indicates that a "tail" exists in the profile.

approach to equilibrium of some non-equilibrium point defect population. It must be understood, however, that this cannot be a simple excess of vacancies or interstitials, as might occur in a quenched metal for example. Point defect energetics in Al_2O_3 have been studied for more than 30 years; the most recent results can be found in refs. 18 and 36. All these studies agree that the defect formation energies are large, about 5 eV per defect. It appears that for intrinsic (pure) crystals, the Schottky quintet is preferred but only by a small margin, and there is disagreement whether the oxygen Frenkel pair is more or less energetic than the Al Frenkel pair. Whatever the case, formation energies of 5 eV per defect are so large that even near the melting point, intrinsic crystals would contain a fractional concentration of only about 10^{-15} point defects. It is clear that the point defects of interest here are the charge-compensating defects necessitated by aliovalent impurities, whether added intentionally or not.

Before discussing this, it is worthwhile to discuss vacancy and interstitial defects in an ionic solid like Al_2O_3 in more detail. Conventionally, our notion of the structure of Al_2O_3 involves a (nearly perfect) *hcp* space-filling structural framework of large oxygen ions, the Al cations occupying 2/3 of the octahedral interstitial sites in an ordered array. Discussion of the structure of Al_2O_3 can be found in many textbooks and articles; a treatment relevant to some of the ideas to follow can be found in a recent article by Heuer et al.³⁷ on the structure of slip and twinning dislocations in Al_2O_3 . The conventional view more or less treats the space filling oxygen sublattice as composed of hard ball-bearing type spheres, which would suggest that vacancy-type defects are more likely than interstitial-type defects. The defect energetics just quoted, however, reveal that the anion-Frenkel pair – an oxygen vacancy and an oxygen interstitial – is a plausible defect in a pure crystal. It must be recognized that oxygen ions are in fact very polarizable,³⁸ and no tracer measurements have been reported that bear on the question whether oxygen diffusion in undoped or impurity-doped sapphire occurs by a vacancy-type or interstitial-type mechanism. The fact that Ti-doping decreases and Mg-doping increases D_{oxy} is of no help, given the "buffering" alluded to above. Simply put, traditional point defect arguments used to interpret activation energies for diffusion in terms of formation and migration enthalpies of the diffusing point defects, either vacancies or interstitials, cannot provide much insight into diffusion phenomena in sapphire.

However, interstitial defects *are* important in sapphire. The best evidence for this can be found in a paper by Phillips et al. dealing with chemical effects accompanying precipitation in Ti-doped sapphire.³⁹ The precipitation of needle-shaped rutile (TiO_2) precipitates is accompanied by formation of large prismatic dislocation loops of interstitial character. The loops climb away from the precipitate–matrix interface during aging, and contain the material that was "plated-out" during precipitation. This plating out process is necessary to accommodate the changes in density and defect population from the (relatively dilute) Ti^{4+} -doped Al_2O_3 solid solution to the (relatively dilute) two phase $\text{Al}_2\text{O}_3 + \text{TiO}_2$ alloy. Detailed analysis³⁹ revealed that the charge compensating defect introduced by the aliovalent Ti^{4+} solute had to involve an oxygen interstitial, O_i'' , rather than an aluminum vacancy, V_{Al}''' . However, this interstitial defect is not

Table 2
Lattice parameters of undoped and Ti-doped sapphire³⁹

	a_o (nm)	c_o (nm)
Undoped Al ₂ O ₃	0.475923	1.249208
Ti-doped Al ₂ O ₃	0.475950	1.299528

a *simple* isolated point defect, even in the dilute alloys that were studied, but must be an interstitial defect complex. This was apparent from the precision lattice parameters that were reported for a crystal doped to a [Ti[•]Al] level of 1×10^{-3} (Table 2).

As can be seen, the lattice expansion due to this (relatively modest) Ti doping is ~ 10 times greater along c than along a . Phillips et al. suggested that an interstitial defect complex containing both Ti and oxygen and elongated along the c axis must be present in the single phase doped solid solution crystal. Whether this suggests that the energy of the oxygen Frenkel defect is preferred in an intrinsic crystal over an Al Frenkel pair, or that the interstitial defect complex in Ti-doped Al₂O₃ is unusually stable, is not yet clear.

Given that anion Frenkel defect pairs are plausible equilibrium defects in an intrinsic crystal, it is equally plausible that oxygen diffusion occurs via an interstitialcy mechanism. Although this mechanism has not figured prominently in the literature dealing with diffusion in oxide ceramics, Ag diffusion in AgBr occurs via this mechanism,⁴⁰ and cation Frenkel disorder does dominate point defect equilibria in this material. An oxygen interstitialcy mechanism would involve a lattice oxygen moving into an interstitial site, and an oxygen interstitial making a correlated jump into the lattice site so vacated (or into a nearby oxygen vacancy). It has relevance to the present problem in the following manner. Assume that defect equilibria in undoped crystals are dominated by quadrivalent impurities. Following the discussion of Ti-doped crystals, it is speculated that such crystals as grown would contain a significant concentration of isolated oxygen interstitials. The processes occurring during annealing would then be the formation of cation-interstitial oxygen complexes of the type responsible for the anisotropic lattice expansion shown in Table 2. There will thus be a decreasing concentration of oxygen interstitials during the ¹⁸O exchange, giving rise to a “tail” in the ¹⁸O penetration profile implied by the unannealed alpha spectrum in Fig. 4, and similar tails determined by SIMS experiments.

Whether this or some other such processes are actually occurring during the annealing that eliminates the non-Fickian behavior must be added to the list of future research questions that require attention.

Before closing this section, it is worthwhile asking how impurity effects – Ti-doping decreasing and Mg-doping increasing D_{oxy} – would be explained if oxygen diffusion occurs by an interstitialcy mechanism. In the former case, the postulated Ti-oxygen interstitial defect complex could provide “blocking” sites. In the latter case, and assuming Mg-doping leads to an increased oxygen vacancy concentration, the jump of an oxygen interstitial into an oxygen vacancy could be facilitated so as to increase D_{oxy} . This is also an interesting topic for future theoretical research.

2.3. Enhanced oxygen diffusion in alumina polycrystals

This section is concerned with enhanced diffusion along grain boundaries in polycrystalline Al₂O₃. There have been four ¹⁸O exchange studies that showed unambiguously that oxygen diffusion was enhanced along grain boundaries in Al₂O₃ compared to bulk or lattice diffusion: papers by Oishi and Kingery,⁴ Reddy,¹⁷ Prot et al.⁴¹ and Nakagawa et al.¹¹ The absence of ¹⁸O concentration profiles in the work of Oishi et al.^{4–6} renders crisp interpretation of diffusion mechanisms difficult if not impossible. The NRA approach of Reddy,¹⁷ the SIMS study of Prot et al.⁴¹ on polycrystals, and the SIMS study of diffusion-bonded bicrystals by Nakagawa et al.¹⁰ avoided this problem. All these researchers assume that the penetration profiles should be plotted as $\log(C - C_{\infty})$ vs. $y^{6/5}$, the Whipple–LeClaire approach.^{42,43} Here, C refers to ¹⁸O surface concentration, C_{∞} the native ¹⁸O concentration (0.204%) and y to penetration. The deeper linear part of such a curve yields the product $D_{b-oxy}\delta$, where D_{b-oxy} is the oxygen grain boundary diffusivity and δ is the grain boundary “width”, i.e. the width of the region where enhanced oxygen diffusion occurs. The initial portion of such a curve provides data on the lattice diffusion coefficient, which is needed to determine $D_{b-oxy}\delta$ values from the slope of the deeper linear portions.

Reddy used four different polycrystals in his work, but only two will be discussed here: undoped hot pressed high purity samples and translucent sintered samples (“Lucalox”) containing 750 ppm MgO. The hot pressed samples were usually annealed for times 5–10 times greater than those used for the diffusion exchange to reduce grain growth during exchange and to “equilibrate” the samples.

For the undoped polycrystals, Reddy used the value for D_{oxy} he had determined on single crystals to determine $D_{b-oxy}\delta$; this was necessary because the penetration depths corresponding to oxygen lattice diffusion were too small to determine D_{oxy} . Since δ is not known, values of $D_{b-oxy}\delta$ are shown in Fig. 5. The Arrhenius parameters of this data are included in Table 1 and Fig. 5.

The ¹⁸O penetration was sufficient in the MgO-doped sintered samples that D_{oxy} could be determined from the fits to the alpha spectra; these data are included in the plot of D_{oxy} for doped single crystals in Fig. 3. It is noteworthy that D_{oxy} is enhanced by $\sim 50\times$ compared to D_{oxy} for his undoped crystals, consistent with the earlier loop shrinkage data¹³ but not with Reddy’s own data on Mg-doped crystals.¹² Presumably, there was sufficient MgO in these polycrystalline samples that MgO evaporation was not an issue. $D_{b-oxy}\delta$ data for Lucalox are also shown in Fig. 5 and do not differ appreciably from $D_{b-oxy}\delta$ determined from ¹⁸O exchange experiments on undoped polycrystalline alumina.

Prot et al.⁴¹ also used the Whipple–LeClaire diffusion equation to determine D_{oxy} and $D_{b-oxy}\delta$ for undoped and 225 mol ppm Y₂O₃-doped alumina polycrystals. Annealing of both types of specimens at elevated temperatures led to “heterogeneous” or “bimodal” grain size distributions. All diffusion samples were annealed for 2 h in air prior to the exchange experiment. Unfortunately, the extent of possible grain growth during this annealing cannot be ascertained from the descriptions in their paper, i.e.

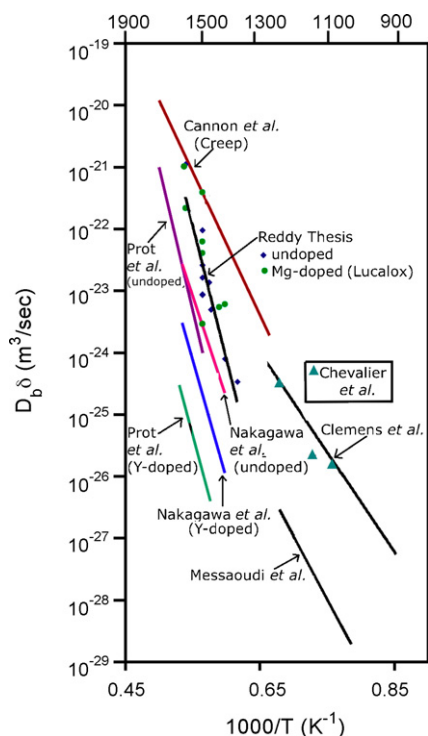


Fig. 5. Oxygen grain boundary diffusion in α - Al_2O_3 .^{11,17,39} Data from creep studies⁵⁶ and sequential oxidation experiments^{46,57,58} are also shown. For the case of Reddy's data,¹⁷ the line shown and the Arrhenius parameters in Table 1 are those for the undoped samples; the Lucalox data fit the line reasonably well. The double oxidation data shown adjacent to the Clemens et al.⁵⁷ curve are from Chevalier et al.⁴⁶ See text for further discussion.

whether the exchanged samples had heterogeneous or bimodal grain size distributions or some other microstructure.

For the undoped samples, the irregular and asymmetrical craters developed during SIMS analysis of ^{18}O penetration profiles prevented D_{Oxy} from being determined, and values deduced for D_{Oxy} from their single crystal data⁹ were used to obtain $D_{\text{b-Oxy}}\delta$ from the penetration plots. This was not a problem for the Y_2O_3 -doped polycrystals.

The $D_{\text{b-Oxy}}\delta$ values for the undoped and Y_2O_3 -doped crystals can be represented by the Arrhenius parameters included in Table 1 and are shown in Fig. 5. There is only tolerable agreement of the undoped polycrystals with the Reddy undoped data. The lower $D_{\text{b-Oxy}}\delta$ values for the Y_2O_3 -doped samples are consistent with the greater creep strength of Y_2O_3 -doped polycrystalline Al_2O_3 ,^{44,45} which has been attributed to Y_2O_3 segregation to grain boundaries, leading to a decrease of $D_{\text{b-Oxy}}\delta$ and retardation of grain boundary dislocation processes (see below and Section 4).

Chevalier et al.⁴⁶ performed a SIMS low temperature ^{18}O exchange study on fine-grained Al_2O_3 polycrystals and reported data on both D_{Oxy} and $D_{\text{b-Oxy}}\delta$. Only five experiments were conducted (an undoped 2.5 μm grain size sample exchanged at 1000 $^\circ\text{C}$, Y_2O_3 -doped polycrystals with a Y/Al ratio of 100 ppm having either 1.5 μm or 2.5 μm grain size, and also exchanged at 1000 $^\circ\text{C}$, and the same two grain size Y_2O_3 -doped samples exchanged at 1200 $^\circ\text{C}$). These data are not included on either Figs. 3 and 5, inasmuch as considerable caution may be needed

with these data because of the very modest penetrations (some nm to tens of nm). Furthermore, both D_{Oxy} and $D_{\text{b-Oxy}}$ are many orders of magnitude larger than those extrapolated from the Prot et al. polycrystalline data. The $D_{\text{b-Oxy}}$ data appears also to be grain size dependent.

Nakagawa et al.¹⁰ used bicrystals for their ^{18}O exchange studies. These were fabricated from high purity Verneuil crystals and contained a $\Sigma 31$ symmetrical tilt boundary ($[0001]$ rotation axis, 17.9 $^\circ$ rotation with regard to $[\bar{1}\bar{1}00]$, $\{7\bar{1}\bar{1}40\}$ grain boundary plane). Pure and Y_2O_3 -doped bicrystals were studied; for yttrium doping, an aqueous solution of yttrium triacetate ($\text{Y}(\text{CH}_3\text{COO})_3$, 0.02 mol/l) was used to coat a polished surface of one of the crystals prior to diffusion bonding. In the language of "complexions" recently advocated by Dillon et al.^{47,48} these boundaries are Type II (undoped) and Type I (Y-doped), respectively.

Their $D_{\text{b-Oxy}}\delta$ data are included in Table 1 and Fig. 5. The undoped data is in good agreement with the undoped data of Prot et al.⁴¹ Nakagawa et al. found that Y_2O_3 -doping decreases $D_{\text{b-Oxy}}\delta$ by a factor of ~ 10 , which is not as large a decrease as was found by Prot et al. (~ 2 orders of magnitude). It is tempting to place considerable credence on these bicrystal data because of the detailed and quite beautiful TEM studies of these boundaries that have been reported.⁴⁹ By way of contrast, there was only meager microstructural characterization devoted to Prot et al. and Reddy's polycrystals. In spite of the fact that only one bicrystal orientation was studied, the Nakagawa et al. data are considered very useful for comparison with high temperature creep data. It is clear, however, that additional studies of bicrystals with different boundary types, including general grain boundaries, would be most helpful.

The mechanism by which Y_2O_3 -doping of bicrystals decreases $D_{\text{b-Oxy}}\delta$ (and Y segregation to grain boundaries in alumina polycrystals increases creep resistance), is not yet clear. Nakagawa et al. suggest either "site blocking", in which Y ions on Al sites in grain boundaries block critical diffusive paths, or a "swamp out" mechanism, in which preferential Y segregation to boundaries prevents segregation of other aliovalent solutes, which would otherwise affect the local point defect populations (oxygen vacancies or oxygen interstitials) in the boundaries and hence enhance $D_{\text{b-Oxy}}\delta$. In view of the "buffering" noted earlier, the "site blocking" explanation is preferred.

However, as emphasized earlier by Harding et al.,¹⁸ the magnitude of the pre-exponential terms from the Prot et al.³⁴ and Reddy¹⁷ grain boundary data are difficult to interpret in terms of basic random walk diffusion theory. D_0 and Q values reported by Nakamura et al. are much lower than those of Prot et al.⁴¹ and Reddy¹⁷; nevertheless, within this data set, Q for $D_{\text{b-Oxy}}\delta$ is higher than Q for D_{Oxy} . Understanding this counterintuitive finding constitutes an equally serious conundrum to those raised earlier for oxygen lattice diffusion.

The difficulty of understanding grain boundary diffusion on fundamental grounds may arise because the transport does not involve simple jumping of vacancies or interstitials in a disordered region adjacent to a grain boundary, but may occur via glide/climb of grain boundary dislocations, grain boundary ledges, and other structural (linear) defects. There is no good

theory for considering transport in grain boundaries using this type of scenario. It is possible that the concept of “complexions” advocated by Dillon et al.⁴⁸ will be able to provide some new insights into grain boundary diffusion and diffusion-controlled creep of Al₂O₃ (Section 4).

2.4. Pipe diffusion

While the “extrinsic” curve of Oishi and Kingery⁴ has subsequently been attributed to dislocation-enhanced diffusion, the poor knowledge of the total surface area of their specimens renders determination of pipe diffusion coefficients difficult. On the other hand, Tang et al.⁵⁰ used an indirect method based on annihilation of dislocation dipoles to determine D_{pipe} . Undoped and 30 ppm Mg-doped sapphire which had been plastically deformed by basal slip ((0001) 1/3 [1120]) to a strain of ~5% at 1375 °C were studied. The dipole breakup process is conservative, in that there is no net flux of point defects between the dipoles and the bulk crystal,⁵¹ so the kinetics of annihilation are controlled by pipe diffusion.

The data for breakup of perfect dipoles in undoped sapphire are included in Table 1 and are plotted in the conventional manner in Fig. 6. (Insufficient pipe diffusion data were available for the Mg-doped crystals to determine an Arrhenius equation, but the diffusion kinetics are about six times faster than for undoped crystals.) While this approach does not permit determination of whether the rate controlling (slower) specie in the pipe diffusion process is that for an oxygen or aluminum point defect, Table 1 and Fig. 6 show that the activation energy is lower than that for lattice diffusion of either specie, which is comforting.

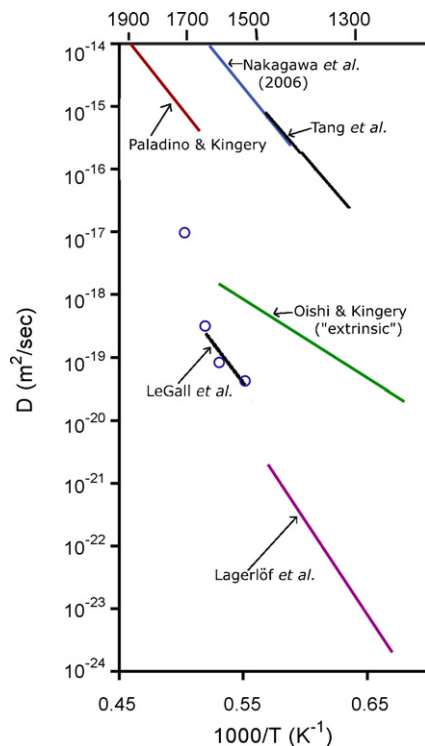


Fig. 6. Al lattice diffusion^{21,55} and pipe diffusion data for α -Al₂O₃.^{50,52} See text for further discussion.

On the other hand, the recent elegant experiment of Nakagawa et al.¹⁰ made clear that oxygen probably is the slower specie in the dislocation pipe diffusion process. They made use of a novel “two-stage deformation” technique that Nakamura et al.⁵² had used to prepare thin plates containing a high density of dislocations, all perpendicular to the plate surface.

Briefly, samples oriented for basal slip were plastically deformed by 5% at 1400 °C, followed by an additional 5% strain at 1200 °C. Under these conditions, a very high dislocation density of $1.1 \times 10^{13} \text{ m}^{-2}$ could be realized, most of which had the edge orientation. Subsequently, thin plates were cut out along the {1100} plane, mechanically ground with diamond paste, ion-milled to achieve a thickness less than 10 μm , and annealed for 30 min in air at 1400 °C. During this annealing, some of the dislocations dipoles present broke up into small prismatic loops,⁵¹ while other dislocations rearranged themselves until they were straight and intersected both surfaces of the thin plates. This dislocation straightening is driven by image forces (the attractive force between the free surface and the strain field of the dislocation) and provided an ideal dislocation substructure for subsequent ¹⁸O exchange experiments.

Samples for the tracer measurements were ground and polished, finishing with a 0.5 μm diamond past and pre-annealed in air for 3 h at 1500 °C. ¹⁸O diffusion exchange experiments were conducted at 1424 °C for 20 h, 1536 °C for 6 h, and 1636 °C for 3 h.

SIMS analyses revealed pronounced tails that could be attributed to pipe diffusion. D_0 and Q parameters are included in Table 1 and Fig. 6; there is (astonishingly) good agreement with the values of D_p determined by Tang, Lagerlöf, and Heuer using the indirect method of breakup of dislocation dipoles. (This agreement was achieved assuming the pipe diameter was 1 nm.)

The magnitude of the pre-exponential for pipe diffusion does not suffer from the large values of the (supposed) subgrain diffusion pre-exponential suggested by the French researchers,^{9,15} which Harding et al.¹⁸ found difficult to rationalize.

2.5. Deformation of single crystals

Pletka et al.⁵³ developed a quantitative work hardening model for high temperature basal deformation of sapphire single crystals. Based on TEM studies of dislocation substructures, work hardening is caused by interaction of the prismatic loops formed by dipole breakup with glide dislocations. A steady state is eventually reached, in which recovery exactly balances work hardening; the recovery involves diffusive annihilation of the prismatic loops, a process controlled by oxygen diffusion. It is thus possible to derive a value for D_{Oxy} from creep or constant strain rate tests, and this has been used by Tohda and Castaing⁵⁴ to derive D_{Oxy} ; their data (not shown here) agree very well with the Cawley et al. data included in Fig. 2. Equally significantly, they found that creep rates, ($\dot{\epsilon}$), were independent of $p\text{O}_2$, and that Mg-doping increased $\dot{\epsilon}$ by a factor of 20–180 and Ti-doping decreased $\dot{\epsilon}$ by a factor of 8–15. The creep activation energies (not included in Table 1) were 562 kJ/mol for undoped material and 581 kJ/mol for Mg-doped material.

3. Aluminum lattice diffusion

In contrast to the extensive literature just reviewed dealing with oxygen diffusion in Al_2O_3 , there have been only two reports of aluminum self-diffusion in Al_2O_3 . The first was Paladino and Kingery's early work⁵⁵ on coarse-grained 130–200 μm polycrystals, and the second a more recent study by Le Gall et al.,²¹ who used Verneuil single crystals. The paucity of data reflects the difficulty involved in determination of aluminum self-diffusion coefficients. The only available tracer is ^{26}Al , which is difficult to produce and hence available in only low activity forms. Further, the half life of ^{26}Al is very long, 7.2×10^5 years, so traditional radiotracer diffusion experiments are difficult in the extreme.

Paladino and Kingery hot pressed ^{26}Al -labeled Al_2O_3 powder against Al_2O_3 discs to form diffusion couples, performed the diffusion anneals in a gas-oxygen furnace, and sectioned the samples by lapping parallel to the original diffusion couple interface. They then determined the activity of the lapped radioactive material, which had to be counted in a low-level controlled background radiation facility. D_{Al} was determined in the temperature range 1670–1905 °C. In retrospect, the Paladino/Kingery experiment should be considered “heroic”. Their data are included in Table 1 and Figs. 1, 2 and 6 and reveals the origin of the long held belief in the ceramics community that D_{Al} is very much greater than D_{Oxy} .

Le Gall et al.²¹ come to a very different conclusion. They had access to a slightly more active form of ^{26}Al than did Paladino and Kingery.⁵⁵ Droplets of a dilute solution of $^{26}\text{AlCl}_3$ in HCl were deposited on the surface of the specimen, neutralized with NH_4OH to form $\text{Al}(\text{OH})_3$, and heated at 350 °C to fix the tracer to the oxide surface. During heating to the temperature of the diffusion anneal, the $\text{Al}(\text{OH})_3$ transformed to Al_2O_3 at ~ 1200 °C. After the diffusion anneal, the penetration profile was determined by mechanical sectioning and counting of the residual activity in the remaining sample. Another heroic experiment, considering that the depth of penetration was a few μm or less.

Actually, Le Gall et al. only performed four experiments, at 1540 °C, 1610 °C, 1650 °C, and 1697 °C. The three lower-temperature ^{26}Al penetration profiles contained “tails” which were interpreted as arising from pipe diffusion in dislocations forming low angle subboundaries. In support of this interpretation, one TEM image was presented, as has already been mentioned in Section 2.2. This of course is the same troublesome interpretation as was offered for the tails on ^{18}O penetration profiles.

On this interpretation, the initial portions of the ^{18}O profiles should then represent lattice diffusion, and Le Gall et al. concluded that D_{Al} was of the same order of magnitude as D_{Oxy} . (The three lower temperature data were used to define the line shown in Fig. 6.) The possibility had earlier¹ been considered that the tails found by Le Gall et al. might actually be due to lattice diffusion rather than to subboundary diffusion, the higher activity zone near the surface then being due to enhanced diffusion in a mechanically damaged region. In such a case, the diffusivities from these experiments would be

close to the Paladino/Kingery values and D_{Al} would indeed be $\gg D_{\text{Oxy}}$.

While this view is tempting, it would require that the Le Gall et al. polishing and annealing left a damaged region that was far more severe than that present in the similar Verneuil crystals used by Prot and Monty for their ^{18}O exchange. This is not a very convincing argument.

Le Gall et al. offer no valid criticism of the Paladino/Kingery data to explain the large differences observed, simply stating that “as the lattice diffusion experiments were determined in polycrystals, the results are doubtful, probably unrepresentative of pure lattice self-diffusion but rather representative of apparent diffusion.” (As noted already, the grain size of the Paladino/Kingery samples were 130–200 μm .)

It may be significant that the highest temperature (1697 °C) Le Gall et al. datum did not show a tail and gave a value of $D_{\text{Al}} \sim 10^2 D_{\text{Oxy}}$ (using the Prot/Monty⁹ value for D_{Oxy} at this temperature). Le Gall et al. interpreted this datum as indicating a greater contribution of subboundary diffusion. It is more likely that the process leading to the non-Fickian profile had been eliminated by the annealing occurring during this high temperature diffusion experiment.

A careful reading of Le Gall et al.²¹ does not lead this writer to the conclusion that $D_{\text{Al}} \sim D_{\text{Oxy}}$, rather than the Paladino/Kingery $D_{\text{Al}}/D_{\text{Oxy}}$ ratio of $\sim 10^3$ or some value in between. On balance, the traditional ceramic view that D_{Al} is $\gg D_{\text{Oxy}}$ is probably correct. This same conclusion had been arrived at earlier when considering the Le Gall et al. data with regard to whether D_{Oxy} or D_{Al} controlled the loop shrinkage data.¹³ Clearly, however, a new study using more active forms of ^{26}Al , which are now available, and SIMS analysis of ^{26}Al concentration profiles, which is also possible, would be most desirable.

4. Diffusional creep in polycrystalline Al_2O_3 and oxidation of Al_2O_3 -scale-forming alloys

Some years ago, Cannon et al.⁵⁶ deduced $D_b\delta$ values for hot pressed and sintered MgO-doped Al_2O_3 from diffusional creep data (Table 1 and Fig. 5); they were convinced that the rate controlling process involved aluminum, rather than oxygen grain boundary diffusion, because the latter was deemed to be very rapid. The comparison of $D_{b-\text{oxy}}\delta$ data with the creep-derived values of $D_b\delta$ (Fig. 5) casts doubt on this assumption.

What else can be said about the atomistic processes dominating creep and oxidation? These high temperature processes are both diffusion-controlled but differ in one essential regard: creep (and sintering) rates for Al_2O_3 are determined by the *slower* specie, aluminum or oxygen, moving on its *fastest* path (through the lattice or along grain boundaries). Al_2O_3 scales resulting from oxidation of Al-containing alloys, on the other hand, are formed by the *faster* specie moving along its *fastest* path.

As noted already, oxygen grain boundary diffusion appears to be decreased by Y-doping,^{11,41} which can be correlated with the increased creep strength of Al_2O_3 polycrystals doped with Y_2O_3 (and ZrO_2 and rare earth oxides).^{44,45} However, mechanistic understanding of this phenomenon is not straight-forward. There is considerable literature on the topic; focus will be given to just

two papers, one from the University of Tokyo group⁴⁴ and one from the Lehigh University group⁴⁵ who have been the most active. The aim here is not to review the extensive literature on diffusion creep in alumina, but to discuss the “Y effect” on both oxygen tracer diffusion and creep.

Yoshida et al.⁴⁴ showed that the creep resistance of fine-grained (~1.0 μm) dense Al₂O₃ polycrystals doped with 0.045 mol% Y₂O₃, La₂O₃, and Lu₂O₃ had creep rates 50–200 times lower than undoped Al₂O₃ at stresses between 10 MPa and 200 MPa and at temperatures between 1150 °C and 1350 °C. Furthermore, as shown in Table 1, the creep activation energy, *Q*, is increased from 410 kJ/mol for the undoped material to 830 kJ/mol for the Y₂O₃-doped samples.

Similarly, Cho et al.⁴⁵ found a similar reduction in creep rate on Y-doping (1000 ppm). Using creep tests at a stress of 50 MPa in the temperature range, 1200–1350 °C, *Q* was determined to be 483 kJ/mol for undoped alumina and 685 kJ/mol for Y-doped material.

Both groups found that creep of fine-grained alumina could be described by the familiar empirical equation

$$\dot{\epsilon} = A\sigma^2 \exp\left(\frac{-Q/RT}{d^3}\right) \quad (1)$$

where $\dot{\epsilon}$ is the strain rate under a stress σ , *A* is a constant, *d* is the grain size and *RT* has its usual meaning. (The Lehigh data⁴⁵ were normalized to a grain size of 2.4 μm using Eq. (1)) The σ^2/d^3 strain rate dependence is usually interpreted as arising either from “interface-reaction controlled” diffusional creep or grain boundary sliding. Whatever the mechanism, it is now clear that Y-doping decreases the creep rate and increases the creep activation energy much more than Y-doping decreases oxygen grain boundary diffusivity and increases *Q* for *D*_{b-ox}. The Y effect thus must involve more than simple retardation of grain boundary diffusion.

The important implication is that creep requires grain boundary diffusion and grain boundary sliding. This should not be surprising—“pure” diffusional creep requires $\dot{\epsilon} \sim \sigma/d^2$ or $\dot{\epsilon} \sim \sigma/d^3$ (Nabarro–Herring and Coble creep, respectively). The nature of the grain boundary ledges or grain boundary dislocations that gives rise to the σ^2/d^3 creep equation, if they are involved in the creep mechanism, is an important question in ceramic science; in fact, the issue of non-Newtonian creep, $\dot{\epsilon} \sim \sigma^n$, *n* > 1, was raised as early as 1980 in the Cannon et al. paper.⁵⁶ It needs resolution!

A final comment. Absent tracer data on aluminum grain boundary diffusion, it is not possible to determine with certainty whether creep in undoped or Y₂O₃-doped fine-grained Al₂O₃, is controlled by oxygen or aluminum grain boundary diffusion.

The situation with regard to oxidation of Al-containing alloys is, if anything, even worse. Temperatures of interest are lower (900–1200 °C) than those for creep or sintering, (or that have generally been used in measuring oxygen and aluminum diffusivities in Al₂O₃). The literature is much too voluminous to attempt anything but a brief summary here. It is generally agreed that transport through growing Al₂O₃ scales occurs predominantly by inward oxygen grain boundary diffusion, but that a non-trivial amount (say 5–10% of total scale growth) occurs

by concurrent outward aluminum diffusion, also along grain boundaries. These transport issues have many implications for oxidation-induced stresses; unfortunately, space does not permit adequate discussion here.

Attention is restricted to three papers^{46,57,58} which attempt to extract *D*_{b-ox}δ data from so-called double oxidation experiments, in which oxidation in ¹⁶O₂ ambients is followed by further oxidation in ¹⁸O₂, with the final ¹⁸O distribution in the scales being determined by SIMS.

Clemens et al.⁵⁷ studied MA956, an oxide-dispersion strengthened (ODS) ferritic alloy containing (in wt%) Fe–20 Cr–4.5 Al–0.3 Ti–0.5 Y₂O₃ oxidized between 900 °C and 1200 °C. Both *D*_{oxy} and *D*_{b-ox}δ could be determined by combining careful analyses of oxide growth rates, scale microstructures, and SIMS depth profiling to determine ¹⁶O/¹⁸O ratios through the scales. The *D*_{b-ox}δ data is shown in Table 1 and Fig. 5 (these authors actually published *D*_{b-ox} data but gave sufficient detail that *D*_{b-ox}δ could be determined).

Their analysis is such that *D*_{oxy} is the only free parameter; the value they determined at 1100 °C, 1×10^{-20} m²/s, is about 3 orders of magnitude higher than the extrapolated lattice diffusion data from the earlier loop shrinkage work.¹³ (This comparison with loop shrinkage data is appropriate because the *D*_{oxy} data so determined were measured down to a lower temperature (1250 °C) than any of the cited studies that have measured *D*_{oxy} using ¹⁸O tracers.) This discrepancy may be related to incorporation of some Fe and Cr into the Al₂O₃ scale, as Fe₂O₃ and Cr₂O₃ additions are known to increase creep rates of polycrystalline Al₂O₃.⁵⁹ It must be recognized, however, that correlation of diffusivities determined or inferred from oxidation experiments with those determined from diffusion experiments has traditionally been difficult.

This same alloy was studied by Messaoudi et al.⁵⁸ using a very similar approach. Their *D*_{b-ox}δ data are included in Table 1 and Fig. 5 and are about 2 orders of magnitude lower than those reported by Clemens et al.⁵⁷ This difference was attributed by Messaoudi et al. to the Clemens et al. analysis ignoring the possibility of outward cation diffusion and the effect of surface roughness on their analysis. Whatever the issue, extrapolated *D*_{b-ox}δ data of Prot et al.,⁴¹ Reddy,¹⁷ and Nagakawa et al.¹¹ would be 1–2 orders of magnitude lower still.

Chevalier et al.⁴⁶ used two model steel alloys, Fe–20 Cr–5 Al and Fe–20 Cr–5 Al–0.1 Y, sequential double oxidation, and SIMS analysis of ¹⁸O concentration profiles. Their Y-free *D*_{oxy} data are included in Fig. 5 and agree well with the ODS data of Clemens et al.⁵⁷ *D*_{b-ox}δ data for the Y-containing alloy at 1100 °C were 3000 times lower than the data shown on Fig. 5 but still higher than the extrapolated Prot et al.⁴¹ and Nakagawa et al.¹⁰ Y-doped data. One conclusion is that Y₂O₃ incorporated in ODS ferritic alloys does not appear to have the same effect on oxidation as Y incorporated directly into the alloy.

More significantly, the lack of agreement between *D*_{b-ox}δ deduced from sequential double oxidation experiments involving ¹⁸O, and *D*_{b-ox}δ determined by ¹⁸O exchange in Al₂O₃ polycrystals has interesting implications. Could it be that the Al₂O₃ grain boundaries have a different structure (and possibly a different chemistry) at the oxidation temperatures of

interest, 900–1200 °C, than they do at higher temperatures where creep and diffusion experiments on Al₂O₃ polycrystals are performed? If this is the case, ceramic scientists may have little to offer high temperature corrosion scientists regarding transport processes through alumina scales.

5. Concluding remarks

We really do not understand a great deal about oxygen and aluminum diffusion in aluminum oxide. The following questions and issues have been identified in this review:

- (i) What is the nature of the buffering that makes D_{Oxy} in Al₂O₃ single crystals so (relatively) insensitive to impurities, even intentionally added aliovalent dopants?
- (ii) What process(es) are occurring during annealing of single crystal specimens that eliminate non-Fickian behavior? (Although the effect of annealing has been demonstrated in NRA¹⁰ data, it is assumed that annealing would eliminate the tails observed by the French researchers^{9,15,21} in their SIMS studies.) In this regard, TEM studies of the removal of surface damage induced by diamond polishing by annealing would be welcome.
- (iii) How should the sizeable oxygen lattice diffusion activation energies (~530 to ~675 kJ/mol) be interpreted?
- (iv) Is it possible that some previously unconsidered oxygen point defect species such as peroxide or (OH)⁻ ions are important in oxygen diffusion?
- (v) Does oxygen diffusion occur by an interstitialcy mechanism? Are the observed doping effects consistent with this mechanism?
- (vi) Is the ratio of lattice diffusivity for aluminum and oxygen, $D_{\text{Al}}/D_{\text{Oxy}}$, equal to ~10³, ~5, or some number in between? A recent study of aluminum diffusion in mullite⁶⁰ utilized a more active source of ²⁶Al (30 times greater activity than used in ref. 21) and SIMS analysis of the penetration profiles. A similar study of aluminum diffusion in single crystal Al₂O₃ with simultaneous exchange with an ¹⁸O-enriched source, might be able to answer this question.
- (vii) There have been no studies of aluminum diffusion in fine-grained Al₂O₃ polycrystals. Studies similar to those just suggested for aluminum lattice diffusion would be able to ascertain whether aluminum grain boundary diffusion is greater than or smaller than oxygen grain boundary diffusion.
- (viii) The activation energy for oxygen grain boundary diffusion is larger than that for lattice oxygen diffusion, contrary to what is found in metals. Is this because the enhanced grain boundary diffusion involves glide/climb of grain boundary dislocations and other structural defects, rather than enhanced diffusive jumping of point defects in the “disordered” regions adjacent grain boundaries? If this is the case, enhanced diffusion by this mechanism needs to be modeled, recognizing that temperature-dependent transformations in grain boundary structure may be occurring. These studies

may also shed light on why high temperature corrosion scientists have been able to derive so little insight on transport issues controlling Al₂O₃ scale formation from the tracer diffusion studies considered in this review.

Note added in proof

Fielitz et al.⁶¹ performed simultaneous ¹⁸O and ²⁶Al tracer diffusion measurements in the temperature range 1230–1500 °C on Ti-doped Al₂O₃ single crystals and demonstrated that D_{Al} is orders of magnitude higher than D_{Oxy} . Extrapolation of their data to the temperature range used by Paladino and Kingery (1670–1905 °C) reveals very good agreement with the absolute magnitude of D_{Al} , although the D_0 and Q parameters differed. Fielitz, et al. report D_0 and Q values of 7.2×10^{-6} m²/s and 375 kJ/mol, respectively, whereas Paladino and Kingery report values of 3.6×10^{-4} m²/s and 482 kJ/mol. If the two data sets are considered together, implying that Paladino and Kingery’s samples were doped with quadrivalent impurities, probably Si⁴⁺, we find D_0 and Q values of 1.5×10^{-5} m²/s and 386 kJ/mol.

Acknowledgements

The writer acknowledges long friendship with Sir Richard Brook, useful conversations with J.D. Cawley on non-Fickian oxygen diffusion, D.B. Hovis, who prepared the figures and Table 1, and J. Castaing, M. P. Harmer, and B. Lesage, who provided useful criticism of an earlier draft of this manuscript. K.P.D. Lagerlöf suggested that peroxide ions might be involved in oxygen transport, while G. Wei (Osram Sylvania) suggested that (OH)⁻ ions might be important. K.P.R. Reddy encouraged publication of the diffusion data on polycrystalline Al₂O₃ from his Ph.D. thesis.

References

1. Heuer, A. H. and Lagerlöf, K. P. D., Oxygen self-diffusion in corundum (α-Al₂O₃): a conundrum. *Philos. Mag. Lett.*, 1999, **79**, 619–627.
2. Catlow, C. R. A., James, R., Macknott, W. C. and Stewart, R. F., Defect energetics in α-Al₂O₃ and rutile TiO₂. *Phys. Rev. B*, 1982, **25**, 1006–1026.
3. Jacobs, P. W. M. and Kotomin, E., Defect energies for pure corundum and for corundum doped with transition metal ions. *Philos. Mag.*, 1993, **68**, 695–709.
4. Oishi, Y. and Kingery, W. D., Self-diffusion of oxygen in single crystal and poly-crystalline aluminum oxide. *J. Chem. Phys.*, 1960, **33**, 480–486.
5. Oishi, Y., Ando, K. and Kubota, Y., Self-diffusion of oxygen in single crystal alumina. *J. Chem. Phys.*, 1980, **73**, 1410–1412.
6. Oishi, Y., Ando, K., Suga, N. and Kingery, W. D., Effect of surface condition on oxygen self-diffusion coefficients for single crystal Al₂O₃. *J. Am. Ceram. Soc.*, 1983, **66**, c130–c131.
7. Reed, D. J. and Wuensch, B. J., Ion-probe measurement of oxygen self-diffusion in single crystal Al₂O₃. *J. Am. Ceram. Soc.*, 1980, **63**, 88–92.
8. Cawley, J. D., Halloran, J. W. and Cooper, A. R., Oxygen tracer diffusion in single crystal alumina. *J. Am. Ceram. Soc.*, 1991, **74**, 2086–2092.
9. Prot, D. and Monty, C., Self-diffusion in Al₂O₃. II. Oxygen diffusion in “undoped” single crystals. *Philos. Mag. A*, 1996, **73**, 899–917.
10. Nakagawa, T., Nakamura, A., Sakaguchi, I., Shjibata, N., Lagerlöf, K. P. D., Yamamoto, T. et al., Oxygen pipe diffusion in sapphire basal dislocations. *J. Ceram. Soc. Jpn.*, 2006, **114**, 1013–1017.

11. Nakagawa, T., Sakaguchi, I., Shibata, N., Matsunaga, K., Mizoguchi, T., Yamamoto, T. *et al.*, Yttrium doping effect on oxygen grain boundary diffusion in Al_2O_3 . *Acta Mater.*, 2007, **55**, 6627–6633.
12. Reddy, K. P. R. and Cooper, A. R., Oxygen diffusion in sapphire. *J. Am. Ceram. Soc.*, 1982, **65**, 634–638.
13. Lagerlöf, K. P. D., Mitchell, T. E. and Heuer, A. H., Lattice diffusion kinetics in undoped and impurity-doped sapphire ($\alpha\text{-Al}_2\text{O}_3$): a dislocation loop annealing study. *J. Am. Ceram. Soc.*, 1989, **72**, 2159–2171.
14. Cawley, J. D. and Halloran, J. W., Dopant distribution in nominally yttrium-doped sapphire. *J. Am. Ceram. Soc.*, 1986, **69**, C195–C196.
15. Le Gall, M., Huntz, A. M., Lesage, B. and Monty, C., Self-diffusion in $\alpha\text{-Al}_2\text{O}_3$ III oxygen diffusion in single crystals doped with Y_2O_3 . *Philos. Mag.*, 1996, **73**, 919–934.
16. Haneda, H. and Monty, C., Oxygen self-diffusion in Magnesium- or Titanium-doped alumina single crystals. *J. Am. Ceram. Soc.*, 1989, **72**, 1153–1157.
17. Reddy, K. P. R., *Oxygen diffusion in close packed oxides*, Ph.D. thesis, Case Western Reserve Univ., Cleveland, OH, 1979.
18. Harding, J. H., Atkinson, K. J. W. and Grimes, R. W., Experiment and theory in alumina. *J. Am. Ceram. Soc.*, 2003, **86**, 554–559.
19. Doremus, R. H., Oxidations of alloys containing aluminum and diffusion in Al_2O_3 . *J. Appl. Phys.*, 2004, **95**, 3217–3222.
20. Doremus, R. H., Diffusion in alumina. *J. Appl. Phys.*, 2006, **100** [101301-1-17].
21. Le Gall, M., Lesage, B. and Bernardini, J., Self-diffusion in Al_2O_3 . I. Aluminum diffusion in single crystals. *Philos. Mag.*, 1994, **70**, 761–773.
22. Pint, B. A. and Deacon, R. M., Comment on “Oxidation of alloys containing aluminum and diffusion in Al_2O_3 ” [J. Appl. Phys. 95, 3217 (2004)]. *J. Appl. Phys.*, 2005, **97** [116111-1-3].
23. Doremus, R. H., Reply to “Comment by Pint and Deacon on ‘Oxidation of alloys containing aluminum and diffusion in Al_2O_3 ’” [J. Appl. Phys. 97, 116111 (2005)]. *J. Appl. Phys.*, 2005, **97**, 116112.
24. Deal, B. E. and Groves, A. S., General relationship for the thermal oxidation of silicon. *J. Appl. Phys.*, 1965, **36**, 3770.
25. Doremus, R. H., Oxidation of silicon by water and oxygen and diffusion in fused silica. *J. Phys. Chem.*, 1976, **80**, 1773–1775.
26. Lou, V. L. K., Mitchell, T. E. and Heuer, A. H., Review—graphical displays of thermodynamics of high-temperature gas–solid reactions and their application of oxidation of metals and evaporation of oxides. *J. Am. Ceram. Soc.*, 1985, **68**, 49–58.
27. Lagerlöf, K. P. D. and Grimes, R. W., The defect chemistry of sapphire ($\alpha\text{-Al}_2\text{O}_3$). *Acta Mater.*, 1998, **46**, 5680–5770.
28. Chien, F. R. and Heuer, A. H., Lattice diffusion kinetics in Y_2O_3 -stabilized cubic ZrO_2 single crystals: a dislocation loop annealing study. *Philos. Mag. A*, 1996, **73**, 681–697.
29. Kilo, M., Borchardt, G., Weber, S. V., Scherrer, S. and Tinschert, K., Zirconium and calcium tracer diffusion in stabilized cubic zirconia. *Ber. Buns.-Ges. Phys. Chem.*, 1997, 1361–1365.
30. Hockey, B. J., Plastic deformation of aluminum oxide by indentation and abrasion. *J. Am. Ceram. Soc.*, 1971, **54**, 223–231.
31. Reisman, A., Berkenblit, M., Cuomo, J. and Chan, S. A., The chemical polishing of sapphire and MgAl spinel. *J. Electrochem. Soc.*, 1971, **118**, 1653–1657.
32. Vandimian, R. G., The chemical polishing and etch pitting of sapphire. *J. Electrochem. Soc.*, 1971, **118**, 1804–1809.
33. Cawley, J. D., L’Hoir, A. and Schmaus, D., Characterization of the near-surface region of single crystal alumina diffusion samples using Rutherford back scattering and channeling. *J. Am. Ceram. Soc.*, 1985, **68**, 663–667.
34. Inkson, B. J., Dislocations twinning activated by abrasion of Al_2O_3 . *Acta Mater.*, 2000, **48**, 1883–1895.
35. Saito, T., Hirayama, T., Yamamoto, T. and Ikuhara, Y., Lattice strain and dislocations in polished surfaces on sapphire. *J. Am. Ceram. Soc.*, 2005, **88**, 2277–2285.
36. Matsunaga, K., Tanaka, T., Yamamoto, T. and Ikuhara, Y., First principle calculations of intrinsic defects in Al_2O_3 . *Phys. Rev. B*, 2003, **68** [085110-1-9].
37. Heuer, A. H., Lagerlöf, K. P. D. and Castaing, J., Slip and twinning dislocation in sapphire ($\alpha\text{-Al}_2\text{O}_3$). *Philos. Mag.*, 1998, **78**, 747–763.
38. Finnis, M. W., private communication, 1998.
39. Phillips, D. S., Mitchell, T. E. and Heuer, A. H., Precipitation in star sapphire: III. Chemical effects accompanying precipitation. *Philos. Mag.*, 1980, **42**, 417–432.
40. Shewmon, P. G., *Diffusion in Solids*. McGraw-Hill Book Company, New York, 1963, pp. 151–155.
41. Prot, D., Le Gall, M., Lesage, B., Huntz, A. M. and Monty, C., Self-diffusion in $\alpha\text{-Al}_2\text{O}_3$. IV. Oxygen grain-boundary self-diffusion in undoped and yttria-doped alumina poly-crystals. *Philos. Mag. A*, 1996, **73**, 935–949.
42. Whipple, R. T., Concentration contours in grain boundary diffusion. *Philos. Mag. A*, 1954, **45**, 1225–1230.
43. Le Claire, A. D., The analysis of grain boundary diffusion measurements. *Br. J. Appl. Phys.*, 1963, **14**, 351–356.
44. Yoshida, H., Ikuhara, Y. and Sakuma, T., High-temperature creep resistance in rare-earth-doped fine-grained Al_2O_3 . *J. Mater. Res.*, 1998, **13**, 2597–2601.
45. Cho, J., Wang, C. M., Chan, H. M., Rickman, J. M. and Harmer, M. P., Role of segregating dopants on the improved creep resistance of aluminum oxide. *Acta Mater.*, 1999, **47**, 4197–4207.
46. Chevalier, S., Lesage, B., Legnos, C., Borchardt, G., Stnehl, G. and Kilo, M., Oxygen diffusion in alumina. Applications to synthetic and thermally grown Al_2O_3 . *Defect Diffusion Forum*, 2005, **237–40**, 899–910.
47. Dillon, S. J. and Harmer, M. P., Multiple grain boundary transition in ceramics: a case study of alumina. *Acta Mater.*, 2007, **55**, 5247–5254.
48. Dillon, S. J., Tang, M., Carter, W. C. and Harmer, M. P., Complexion: a new concept for kinetic engineering in material science. *Acta Mater.*, 2007, **55**, 6208–6218.
49. Bubanm, J. P., Matsunaga, K., Chen, J., Shibata, N., Ching, W. Y., Yamamoto, T. *et al.*, Grain boundary strengthening in alumina by rare earth impurities. *Science*, 2006, **311**, 212–215.
50. Tang, X., Lagerlöf, K. P. D. and Heuer, A. H., Determination of pipe diffusion coefficients in undoped and magnesia-doped sapphire ($\alpha\text{-Al}_2\text{O}_3$): a study based on annihilation of dislocation dipoles. *J. Am. Ceram. Soc.*, 2003, **86**, 560–565.
51. Lagerlöf, K. P. D., Mitchell, T. E. and Heuer, A. H., Energetics of the break-up of dislocation dipoles into prismatic loops. *Acta Met.*, 1989, **37**, 3515–3525.
52. Nakamura, A., Lagerlöf, K. P. D., Matsunaga, K., Tohma, J., Yamamoto, T. and Ikuhara, Y., Control of dislocation configuration in sapphire. *Acta Mater.*, 2005, **53**, 455–462.
53. Pletka, B. J., Heuer, A. H. and Mitchell, T. E., Work hardening in sapphire ($\alpha\text{-Al}_2\text{O}_3$). *Acta Met.*, 1977, **25**, 25–33.
54. Tohida, H. and Castaing, J., Oxygen diffusion and its relation to high temperature deformation of ceramic oxides. In *Lattice Defects in Ceramics*, eds. J. Castaing, A. Dominguez-Rodriguez, C. Monty, 1989, JJAP Series 2, pp. 97–103 [unpublished results quoted].
55. Paladino, A. E. and Kingery, W. D., Aluminum ion diffusion in aluminum oxide. *J. Chem. Phys.*, 1962, **37**, 957–962.
56. Cannon, R. M., Rhodes, W. H. and Heuer, A. H., Plastic deformation of fine-grained alumina (Al_2O_3): I. Interface-controlled diffusional creep. *J. Am. Ceram. Soc.*, 1980, **63**, 46–53.
57. Clemens, D., Bongartz, K., Quadackers, W. J., Nickel, H., Holzbrecher, H. and Brecker, J. S., Determination of lattice and grain boundary diffusion coefficients in protective alumina scales on high temperature alloys using SEM, TEM, and SIMS. *Fresenius’ J. Anal. Chem.*, 1995, **353**, 267–270.
58. Messaoudi, K., Huntz, A. M. and Lesage, B., Diffusion and growth mechanisms in Al_2O_3 scales on kinetic Fe–Cr–Al alloys. *Mater. Sci. Eng. A*, 1998, **247**, 248–262.
59. Lessing, P. A. and Gordon, R. S., Creep of polycrystalline alumina, pure and doped with transition metal impurities. *J. Mater. Sci.*, 1977, **12**, 2291–2302.
60. Fielitz, P., Borchardt, G., Schmucker, M. and Schneider, H., Al-26 diffusion measurement in 2/1-mullite by means of secondary ion mass spectrometry. *Solid State Ionics*, 2006, **177**, 493–496.
61. Fielitz, P., Borchardt, G., Ganschow, G., Bertram, R. and Markwitz, A., Al-26 tracer diffusion in titanium doped single crystalline $\alpha\text{-Al}_2\text{O}_3$. *Solid State Ionics*, submitted.